Stress or Strain Does Not Impact Sorption in Stiff Mesoporous Materials

M. Bossert, A. Grosman, I. Trimaille, C. Noûs, Etienne Rolley

Stress or strain does not impact sorption in stiff mesoporous materials

M. Bossert, A. Grosman, I. Trimaille,[1] C. Noûs,[2] and E. Rolley[3,*]

[1]*Sorbonne Université, CNRS, Institut des NanoSciences de Paris, INSP, F-75005 Paris, France*

[2]*Laboratoire Cogitamus 1 3/4 rue Descartes, 75005 Paris*

[3]*Laboratoire de Physique de l'Ecole Normale Supérieure, ENS, Université PSL, CNRS, Sorbonne Université, Université de Paris, F-75005 Paris, France*

Abstract

The present paper investigates strain-induced sorption in mesoporous silicon. Contrarily to a previous report based on indirect evidence, we find that external mechanical strain or stress has no measurable impact on sorption isotherms, down to a relative accuracy of 10^{-3}. This conclusion is in agreement with the analysis of sorption-induced strain of porous silicon, and holds for other stiff mesoporous materials such as porous silicas.

INTRODUCTION

The deformation of a porous material upon fluid adsorption has attracted much interest for a long time because of its importance in many situations such as drying of concrete, swelling of coal and shale. Recently, the adsorption-induced strain has been measured for various nanoporous or microporous materials (see recent reviews by Gor et al. [1] and Vandamme [2]). At low vapor pressure, contraction or swelling may occur due to the competition between the attraction of adsorbed molecules to the pores walls and the packing effects; close to saturation pressure, swelling is usually observed. When the strains induced by adsorption are small, the calculation of the pressure in the fluid and the resulting strain of the solid skeleton can be uncoupled. In this limit, a thermodynamic approach based on the Derjaguin–Broekhoff–de Boer theory successfully accounts for the strain measured for instance in mesoporous silica [3], while non-linear density functional theory (NLDFT) is needed to describe the strain of microporous materials like zeolites [4]. Molecular dynamics is an alternative to NLDFT [5] and allows to take into account the coupling between the fluid adsorption and the porous network deformation [6, 7]. The basic mechanisms responsible for adsorption-induced strain are now well understood in a variety of materials (see [1] for further references).

As stressed by Vandamme [2], if adsorption deforms a solid, deformation should impact the sorption process, whatever the nature of the fluid, the pore size or the pore network geometry. This reverse process has only recently been investigated. For systems presenting a strong adsorption-induced deformation, the reverse process is easily observed in polymers [8], metal-organic framework [9] and aerogels [10]. For coal, a much stiffer system for which the adsorption-induced strain is of order 10^{-2}, the impact of an external stress on adsorption has also been quantitatively demonstrated [11].

Here, we are interested in still stiffer systems such as porous silica or porous silicon. For these materials, following the pioneering work of Amberg and McIntosh on disordered porous silica [12], the interest in adsorption-induced strain has recently triggered many studies [13–16]. For such mesoporous materials, the maximal strain due to adsorption is of the order of 10^{-3}, a small value which explains why the reverse impact of an external stress on fluid sorption is usually neglected.

However, in a intriguing work, Grosman and Ortega [17] have observed that the sorption isotherms of nitrogen in porous silicon are shifted for porous samples still attached to the underlying silicon wafer with respect to free standing porous membranes. They explained that this shift was likely to be due to the stress in the supported sample, caused by the lattice mismatch between porous and bulk silicon [18]. They further argued [19] that the coupling between mechanics and adsorption could be responsible for inter-pore coupling. has triggered a renewed interest in the role of surface stress in the strain-adsorption coupling, pointed long ago by Eriksson [20] (an illuminating discussion can be found in a recent article by Gor and Bernstein [21]). However, the relevance of surface stress in porous silicon is still controversial [22, 23], and more generally, the amplitude and the possible consequences of strain-induced adsorption in stiff mesoporous materials is still an open question.

In the present paper, we report on experiments designed specifically to settle this point. We have designed two different setups which allow to control either the strain or the stress of a *single* porous silicon sample. In both cases, we find that the change in the sorption isotherms is below the experimental resolution. We show that this conclusion is actually consistent with earlier measurements of adsorption-induced strain [13, 24]. The apparent discrepancy between the present experimental results and the observations by Grosman and Ortega could be due to the fact that they compare the sorption in *different* samples. The difference in fabrication processes between supported samples and free membranes could cause a small change in the structure of the porous layers, hence some changes in the sorption isotherms. Finally, we discuss the amplitude of stress-induced adsorption in other materials and show that these effects are negligible for stiff mesoporous materials such as porous silicas.

MATERIALS AND METHODS

Porous silicon samples. The preparation process, the morphology, and the physical properties of p+-type porous silicon have been reported elsewhere [25] so that we give here only a brief outline of these properties. In particular, the determination of pore size distribution from electron microscopy imaging is reported in detail in ref. [25]. Porous silicon is obtained by anodic dissolution of highly boron doped (100) Si single crystal in hydrofluoric acid solution. The pores are perpendicular to the wafer surface. The pore cross sections have a polygonal shape, with a broad pore size distribution, which depends on the

etching conditions: for a nominal porosity of 50%, the transverse dimension of the pores is $\langle d \rangle = 13$ nm, with $7 < d < 20$ nm. For a nominal porosity of 70%, $\langle d \rangle = 26$ nm, with $12 < d < 40$ nm.

It has been shown [25], that the porosity is invariant along the pore axis and independent on the thickness of the porous layer. However, recent measurements of diffusion constants along and transverse to the the pore axis suggest that there are some connections between neighboring pores and also some constriction along the pores [26, 27].

At the end of the preparation process, once the desired thickness (*i.e.* pore length) is reached, the anodic current can be switched off to produce a *supported porous layer* attached to the Si substrate (Fig 1b). Alternatively, the current can be increased to dissolve the Si walls at the bottom of the pores. One thus obtains a free standing *porous membrane* (Fig 1a). In this work, the thickness of the membranes is 20 or 50 μm, that of the supported layers ranges from 4 to 20 μm. We also used a third geometry, where the upper porous layer lies on an intermediate layer of higher porosity, and hence softer, attached to the silicon substrate (Fig. 1c). This *duplex* geometry is achieved by changing the etching parameters [28]. In this case, the mechanical coupling between the upper layer (the layer of interest) and the substrate is intermediate between a membrane and a supported layer, and this coupling can be tuned by changing the thickness (6 to 60 μm) of the intermediate layer.

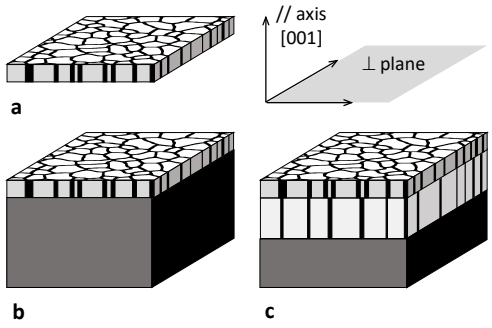

FIG. 1. Geometry of the samples: free membrane (a), supported layer (b) and duplex layer (c). In the later case, the porous layer of interest is the upper one.

In all cases, we note $\epsilon_{\parallel}$ and $\sigma_{\parallel}$ the components of the strain and stress tensor along the pore axis (fig. 1). Porous silicon is a transverse isotropic material [24]: when samples are submitted to a biaxial transverse stress, the transverse strain $\epsilon_{\perp}$ and stress $\sigma_{\perp}$ are invariant through any rotation around the pore axis.

Sorption isotherms. Sorption experiments are performed at $T = 18°C$, the fluids used being n-hexane or n-heptane. Admission of fluid in the cell is controlled with a precision needle valve and the vapor pressure P is measured with a pressure transducer. The cell is equipped with an optical window for measuring either the deformation of the sample or the amount of adsorbed fluid. The later is determined through White Light Interferometry (WLI): when the porous layer is illuminated by a white light beam, the interference between the two beams reflected at both side of the porous layer creates oscillations in the spectrum of the reflected light. The analysis of these oscillations yields the optical thickness L of the layer [29, 30]. In contrast with standard volumetric techniques which require integration of the fluid flow in the cell, L measurement is instantaneous, and the variation of the thickness due to adsorption can be tracked at the acquisition rate of the spectrometer (about 0.1 Hz), so that the optical sorption isotherms L *vs* P appear as continuous curves (see Supplementory Information for details about the setup and the spectrum analysis).

The raw output of WLI is $L = 2n_{eff}\, l_{\|}$, where $l_{\|}$ is the geometrical thickness of the porous layer along the pore axis, which may change slightly along an isotherm, and the effective optical index n_{eff} which depends on the adsorbed amount (mole number N) in the pores. So the change $\Delta L = L(P) - L(0)$ reflects the change in N. Sorption isotherms will be displayed as $\Delta L(P)$, or as the normalized change $\Delta L/\Delta L_M = \Delta L/(L(P_{sat}) - L(0))$ in order to compare samples with different thicknesses (P_{sat} is the saturated vapor pressure). The resolution is limited by small heterogeneities of the samples: changing the mechanical control parameters causes a small displacement of the sample with respect to the illuminating light beam. The relative reproducibility is about 10^{-3}.

Calculating N from ΔL requires first to choose an effective medium model among many [31] and, second, a precise knowledge of many parameters such as the porosity, the optical index of the liquid..., which may change along the isotherm. Here, we have chosen to measure L *vs* N directly for a porous silicon sample (see Appendix). We find that ΔL is proportional to N within a few percent. It means that the shape of an optical isotherm $\Delta L(P)$ is very similar to a true sorption isotherm $N(P)$. More importantly here, the impact of an external mechanical parameter, for instance $\epsilon_{\perp}$, measured by $[N(P, \epsilon_{\perp}) - N(P, 0)]\, /N(P_{sat}, 0)$, is equal within a few percent to the normalized change of the optical thickness $[\Delta L(P, \epsilon_{\perp}) - \Delta L(P, 0)]\, /\Delta L_M$ and the final resolution is still 10^{-3}. This is enough for observing the same effect as Grosman and Ortega, which is of the order

of a few percent [17].

Controlling strain. The strain of the sample is easily controlled when using supported layers. The compliance of the layer is much smaller than that of the underlying substrate, so that the strain of the sample is fixed by the strain of the wafer itself. By bending the wafer to a spherical cap, we could reach biaxial strain $\epsilon_\perp$ up to approximately 10^{-3}.

Controlling stress. In this case, we use 50% porosity membrane of thickness 50 μm. The transverse dimensions are 10×15 mm^2. One short side is glued to a fixed frame and the opposite side is glued to a piezo ceramic bimorph. The stiffness of the bimorph is much smaller than that of the membrane, so that the voltage on the piezo controls the force $\mathbf{F}$ directed along the long side of the membrane, hence the stress $\sigma_\perp$ of the membrane. The bimorph response was calibrated prior to the experiment: the stress can reach about 10 MPa. During the sorption experiment, we measure the strain $\epsilon_\perp$ along $\mathbf{F}$. In this experiment, the aspect ratio is too close to one for the strain to be really unixial, but this will not prevent us from drawing a qualitative conclusion.

RESULTS

Supported layer submitted to controlled strain. We have first investigated the impact of a biaxial strain on sorption isotherms. The result is shown in fig.2 for a layer of 70% porosity, 20 μm thick, and for n-hexane. The blue isotherm corresponds to a supported layer as prepared. Note that because of the lattice mismatch between bulk and porous silicon [18], the residual strain in this reference state is not strictly zero. The red isotherm is measured after changing the biaxal strain by $\epsilon_\perp = 8.3\times10^{-4}$. The two curves are almost perfectly superimposed, the upper bound for $|\Delta L(P,\epsilon_\perp) - \Delta L(P,0)|/\Delta L_M$ is 2×10^{-3}. The change in the position of the hysteresis loop is at most $2\times10^{-3}\,P_{sat}$. These changes are of the order of the reproducibility of the experiment, and one order of magnitude smaller than the effect reported by Grosman and Ortega.

Membrane submitted to controlled stress. In a second step, we have investigated the change in adsorbed amount when a porous sample is submitted to an external stress $\sigma_\perp$, approximately uniaxial. In this experiment, we monitor the average strain $\epsilon_\perp$ as a function of the vapor pressure P for different values of $\sigma_\perp$. Strain isotherms are shown in figure 3, for heptane and a 50% porosity membrane. The shape of these isotherms reflects the changes

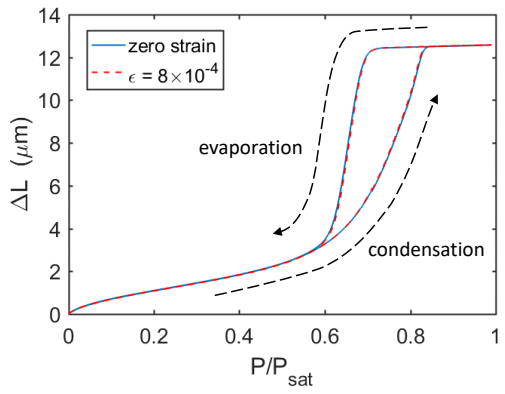

FIG. 2. Optical sorption isotherms for a 70% porosity sample under imposed bixial strain (fluid: hexane). The change ΔL of the optical thickness is plotted as function of the reduced vapor pressure. Changing the transverse strain by 8×10^{-4} has no measurable impact on the isotherm.

in capillary forces along a sorption isotherm and have been discussed in a previous paper [13]. The only effect of applying an external stress $\sigma_\perp = 7$ MPa is to translate the isotherm as a whole. In particular, we find again that the shift in pressure of the hysteresis loop, if any, is smaller than $2 \times 10^{-3}\, P_{sat}$.

As deformations are of the order of a few micrometers, strain measurements are extremely sensitive to a small drift of the relative position of the camera and the experimental cell. This explains why the two strain isotherms do not superimpose as exactly as sorption isotherms in figure 2. In order to look for even a tiny effect of stress on adsorption, we fix the vapor pressure and monitor the amount of adsorbed fluid with WLI when applying an external stress of 7 MPa. As for the strain-controlled experiment, the change in $|\Delta L(P, \sigma_\perp) - \Delta L(P, 0)|/\Delta L_M$ is smaller than the resolution.

DISCUSSION

The experimental results are quite clear: adsorption is not modified when a mechanical control parameter is changed. Before going back to the experiments by Grosman and Ortega, who claimed to observe stress-induced adsorption, it is necessary to check whether the present result is consistent with data on adsorption-induced stress or strain, which has been measured in detail for heptane in poSi. [13, 24].

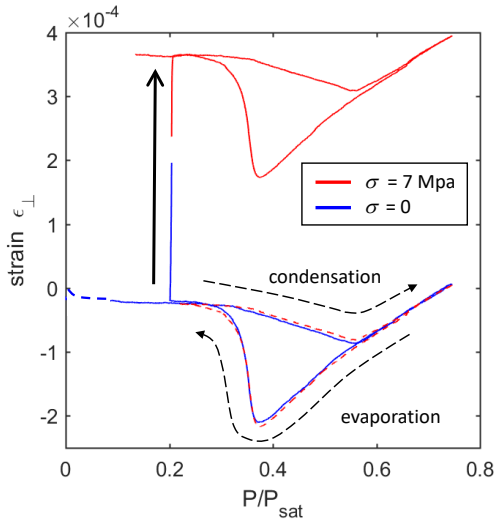

FIG. 3. Strain isotherms for a 50% porosity membrane (fluid: heptane). The strain $\epsilon_\perp$ is measured along the direction of the applied stress $\sigma_\perp$ and is plotted as function of the reduced vapor pressure. A first isotherm (blue line) is recorded at zero stress. After the actuation of the piezo bimorph (thick black arrow), a second isotherm (red line) is recorded for $\sigma_\perp = 7$ MPa. Translating the second isotherm by -3.9×10^{-4} yields the red dashed line: the hysteresis loop occurs at exactly the same pressure for $\sigma_\perp = 0$ and $\sigma_\perp = 7$ MPa.

Back to thermodynamics

As we are not interested here in the details of adsorption at the pore scale, we follow the simple thermodynamic approach by Brochard et al. [32]. The system we consider is the elastic porous matrix and the fluid inside the pores, in isothermal condition.

When the stress $\sigma_\perp$ transverse to the pore axis is biaxial, the strain $\epsilon_\perp$ is the same in any directions perpendicular to the pore direction. Let f be the Helmhotz free energy per unit of undeformed volume. Its differential may be written:

$$df = \sigma_\parallel d\epsilon_\parallel + 2\sigma_\perp d\epsilon_\perp + \mu dn \tag{1}$$

where μ is the chemical potential of the fluid and n is the number of moles of fluid N divided by the volume V_0 of the sample in its reference (undeformed) state. If the stress is uniaxial, perpendicular to the pore axis, df is unchanged except for the factor 2 which disappears in the second term.

Then the Maxwell relations associated with $(f - \mu n)$ yield for instance the variation of

the amount of fluid n as a function of the biaxial strain $\epsilon_\perp$:

$$\left.\frac{\partial n}{\partial \epsilon_\perp}\right|_{\epsilon_\parallel,\mu} = -2 \left.\frac{\partial \sigma_\perp}{\partial \mu}\right|_{\epsilon_\parallel,\epsilon_\perp} \tag{2}$$

Assuming that the gas is perfect, $\mu(P) - \mu(P_{sat}) = RT \ln(P/P_{sat})$. It is more convenient to express μ in term of the pressure $P_L \equiv P_{sat} + \mu/v_L$, where v_L is the liquid molar volume at coexistence. If the liquid is incompressible and for large enough pores, P_L is simply to the liquid pressure in the pores, or the Laplace pressure. Then Eq. 2 may be written:

$$\left.\frac{\partial N}{\partial \epsilon_\perp}\right|_{\epsilon_\parallel,\mu} = -\frac{2V_0}{v_L} \left.\frac{\partial \sigma_\perp}{\partial P_L}\right|_{\epsilon_\parallel,\epsilon_\perp} \tag{3}$$

The quantity that can be derived from the experiment is $(N(P,\epsilon_\perp) - N(P,0))/N_M$ where $N_M = N(P_{sat},0)$. Neglecting the change of volume between the empty sample and the sample at saturation and assuming that the liquid in the pore has the bulk liquid density, $N_M = \phi_0 V_0/v_L$ where ϕ_0 is the porosity in the reference state. Thus we obtain:

$$\frac{N(P,\epsilon_\perp) - N(P,0)}{N_M} = -\frac{2}{\phi_0} \left.\frac{\partial \sigma_\perp}{\partial P_L}\right|_{\epsilon_\parallel,\epsilon_\perp} \epsilon_\perp \tag{4}$$

In the same way, one can compute the change in N when the sample is submitted to a uniaxial stress $\sigma_\perp$:

$$\frac{N(P,\sigma_\perp) - N(P,0)}{N_M} = \frac{1}{\phi_0} \left.\frac{\partial \epsilon_\perp}{\partial P_L}\right|_{\epsilon_\parallel,\sigma_\perp} \sigma_\perp \tag{5}$$

The quantities appearing on the right-hand-side of equations 4 and 5 can be obtained by measuring the mechanical response of a sample along a sorption isotherm. For instance, for a supported porous layer, the biaxial stress in the layer can be calculated from the curvature of the wafer (see ref. [13, 24] for details). Two such stress isotherms $\sigma_\perp$ *vs* P are shown for heptane in figure 4. Computing the response coefficient makes sense only for the reversible regions, below or above the hysteresis loop. In the low pressure regime ($P < 0.05\ P_{sat}$), one finds $\partial\sigma_\perp/\partial P_L|_{\epsilon_\parallel,\epsilon_\perp}$ is about 7×10^{-3} and 3×10^{-3} for 50% and 70% porosity sample, respectively. In the saturation regime, $\partial\sigma_\perp/\partial P_L|_{\epsilon_\parallel,\epsilon_\perp} \simeq -0.2$ and –0.4 for 50% and 70% porosity respectively. These coefficients do not depend on the nature of the fluid [24], so that they can be used either for heptane or hexane. The stress-induced sorption has the opposite sign in the two reversible regions. That reflects the fact that, upon adsorption in a

free sample, contraction is observed at low pressure, while expansion is observed when the sample is saturated [13].

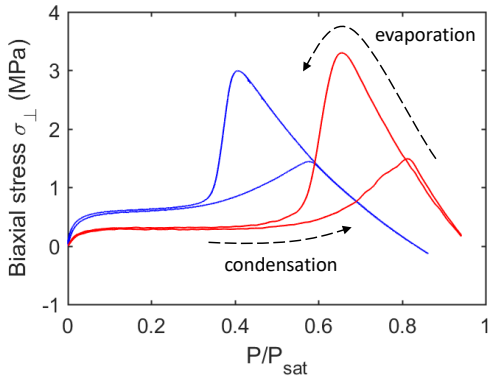

FIG. 4. Transverse bixial stress as a function of normalized vapor pressure (fluid: heptane). Blue: 50% porosity, Red: 70% porosity. The absolute value of $\partial\sigma_\perp/\partial P_L|_{\epsilon_\parallel,\epsilon_\perp}$ is maximum in the mbar region and when the sample is saturated.

Using theses values of the response coefficients and eq. 4, it is straightforward to estimate the impact of a variation of the external strain on the isotherm. In the most favorable case (70% porosity, saturated sample), $(N(P,\epsilon_\perp) - N(P,0))/N_M \sim \epsilon_\perp$: the amount of fluid at saturation should increase very slightly when the porous layer is stretched, but the magnitude of the effect is comparable to the resolution, even for the highest strain we can achieve. In the reversible low pressure region of the isotherms, the shift in N is roughly two order of magnitude smaller. One finds the same orders of magnitude for stress-induced sorption.
In conclusion, thermodynamics predicts that strain-induced or stress-induced adsorption in porous silicon is too small to be observed, in perfect agreement with the experiments.

Membranes *vs* supported layers

So far, our experiments show that mechanics cannot explain the observation by Grosman and Ortega that adsorption isotherms for a 20 μm thick membrane is shifted compared to a supported layer having the same thickness and same porosity (50%). As this shift was observed only for nitrogen at 77 K, we first checked that it is still present for hexane (fig. 5a). We find that the shift in pressure is about 5% of P_{sat}, similar to that of nitrogen.
We have also used a different strategy in order to vary the coupling between the porous

layer and the wafer progressively: a sublayer with a larger porosiy is etched below the 50% porosity layer of interest (fig. 1c) whose pores are opened at both ends for all the samples. As shown in figure 5b, when the sublayer thickness increases, the hysteresis loop shifts towards higher pressure and there is a small decrease in the adsorbed amount at low pressure.

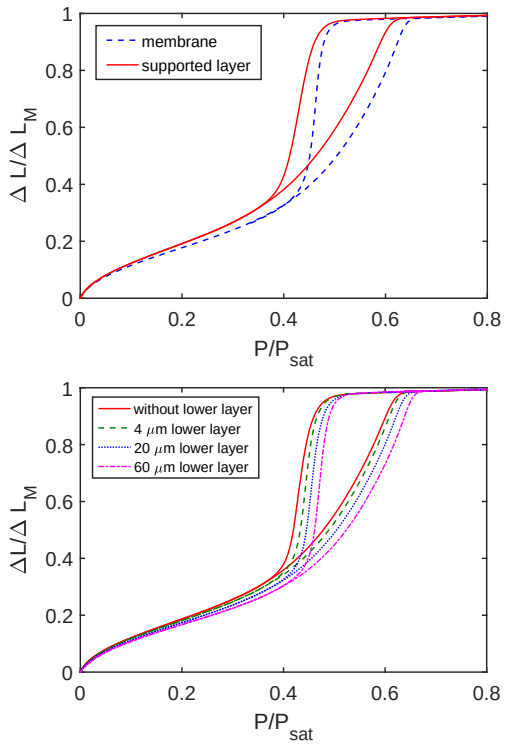

FIG. 5. Normalized optical sorption isotherms for hexane in porous layers (thickness: 20 μm, porosity: 50%). Upper graph: membrane (fig. 1a) vs supported layer (fig. 1c). Lower graph: supported layers with sublayers between the layer of interest and bulk silicon (fig. 1c).

When increasing the sublayer thickness, the variation of the stress in the upper layer is smaller than in the direct experiments described in the previous section, so that a direct mechanical effect can again be ruled out. In this series, the ends of the pores are similar for all the samples so that boundary conditions cannot explain the shift in figure 5b either. The only explanation is that the structure of the upper layer changes as the sublayer grows. The sublayer being etched at constant speed, the upper layer under study is submitted to the electro-etching conditions for a time which increases with the sublayer thickness (in the same way, compared to supported samples, membranes are submitted to a strong current density when they are detached from the substrate). A simple interpretation of the shift of the isotherms would be that the mean transverse dimension of pores increases slightly as a

function on time, due to a small residual dissolution. Using a very crude Kelvin model, for a total etching time of about 1 hour, the 5% shift of the emptying pressure requires a 10% increase of the mean pore diameter. This is not consistent with the fact that the porosity of poSi layers is found to be independent of the thickness [25]. So we rather suspect that the shift is due to a subtle change in the shape of the pore, residual dissolution occurring mainly at some defects at the inner surface of the pores, thus leading to a decrease in the effective diameter of the pore without changing much the porosity. This hypothesis could be checked by high resolution transmission electronic microscopy.

Comparison with other porous materials

The coefficient $\partial\epsilon_\perp/\partial P_L$ appearing in eq. 5 is simply the inverse of the pore load modulus $M_\perp$, which has been measured for many materials. As we are interested here in order of magnitude, let us assume that the material is isotropic, characterized by a single pore modulus M and a bulk modulus K. In this limit, for a sample submitted to an isotropic stress σ eq. 5 reads:

$$\frac{N(P,\sigma) - N(P,0)}{N_M} = \frac{1}{\phi_0}\frac{K}{M}\epsilon_v \tag{6}$$

where ϵ_v is the volumetric strain.

In the context of isotropic microporous materials, the coupling between the volumetric strain ϵ_v and adsorption is rather quantified by a coupling parameter C defined by [32]:

$$\frac{n(\mu,\epsilon) - n(\mu,0)}{n(\mu,0)} = C(\mu)\epsilon_v \tag{7}$$

So the importance of strain-induced sorption (or mechanosorptive effect) depends on the coupling parameter C (or on the quantity $K/(\phi_0 M)$) and on the maximum strain $\epsilon_{v,M}$ that can be achieved.

For a polymeric material, such as cellulose network, $C \sim 10$ [8] and $\epsilon_{v,M} \sim 0.1$, so that the relative change of n is of order 1: the mechanosorptive effect is very large in this type of material. For aerogels, $\phi_0 \sim 1$ and $K \sim M$ [10], so that $C \sim 1$. As aerogels can withstand large strains, stress-induced sorption is still important.

Let us now consider less compliant materials, where the mechanosorptive effect is expected to be smaller. For microporous carbon it is found that $C \sim 10$ and $\epsilon_{v,M} \sim 0.01$ for methane [32] or CO_2 adsorption [11] resulting in a small but measurable coupling.

Data is also available for several type of porous silicas. For microporous silicas, such as faujasite zeolite [4], M is close to K, resulting in C of order 1. This holds also for ordered mesoporous silicas, such as SBA16, MCM41s [14], and for Vycor, a disordered system (see ref. [12, 33] for numerical value of the elastic parameters). For all this materials, the coupling parameter is thus close to the one of porous silicon ($C = 0.3$). As the maximum strain is in the range $10^{-4} - 10^{-3}$, it turns out that, for all this systems, the relative change in the adsorbed amount is 1% at most, below the resolution of standard volumetric and gravimetric techniques.

CONCLUSION

We have designed experiments to measure sorption isotherms of porous silicon, with samples submitted to an external stress or strain. We could not detect any change in the isotherms, in agreement with earlier measurements of sorption-induced strain. It is likely that strain-induced sorption is also negligible for most microporous or mesoporous silicas. As a consequence, we can rule out the proposal by Grosman and Ortega that mechanics is responsible for the difference between isotherms of supported (stressed) or free standing (relaxed) samples of porous silicon. This difference could be due to small changes in the geometry of the pores during the etching process; testing this hypothesis requires a better characterisation of the pore network.

ACKNOWLEDGEMENTS

This paper is dedicated to the memory of our late co-author and colleague A. Grosman. We thank P. Spathis, P.-E. Wolf and J. Puibasset for stimulating discussions and we are indebted to M. Vandamme for clarifying the connection between our measurements and poromechanics. We acknowledge the financial support of Agence Nationale de la Recherche through the project CavConf, ANR-17-CE30-0002, including the funding of M. B.

APPENDIX

Converting the optical thickness L to the amount of fluid N. The output of interferometric measurement is the optical thickness $L = 2n_{eff}l_{\|}$. When using this technique for studying adsorption in porous silicon [29, 34] or porous alumina [30], it is usually assumed that the geometrical thickness $l_{\|}$ does not change upon adsorption. For porous silicon, this is true within a relative accuracy of 10^{-3} [24]. Then, n_{eff} is converted to the fraction g of the pore volume which is occupied by the liquid using a model for the effective medium consisting in 3 phases: silicon, liquid and vapor.

This conversion requires first to chose a model among existing ones (Maxwell Garnet, various Bruggeman models...[31]) and second to know precisely the optical indices of the silicon n_{Si} and of the liquid n_L, as well as the porosity ϕ. Again, the variation of ϕ is small along an isotherm, but that of n_L is not negligible: actually, the change in the optical index of the liquid with P_L is responsible for the slope of the saturation plateau in figure 5. In any case, most models predict a nearly linear dependence in g of the effective optical index n_{eff}. Hence, the optical thickness L should also vary roughly linearly with the amount of fluid N in the pores.

Given the difficulties of the conversion, we have decided to check the relation between L and N. To this end, we have measured L and N independently as a function of the vapor pressure P along a sorption isotherm. The sample was a 50% porosity supported layer, 20 μm thick. The volumetric isotherm $N(P)$ was measured using a commercial apparatus (HPVA II Micromeritics) equipped with a 1000 Torr pressure transducer. The fluid was nitrogen (instead of hexane to avoid any contamination of the apparatus) and the sorption isotherm was measured at 77.4 K. For measuring the optical isotherm $L(P)$ at the same temperature, we built an optical cell that can be attached to a nitrogen dewar (raw isotherms $N(P)$ and $L(P)$ are shown in the Supplementory Information).

As shown in figure 6, the optical thickness L varies linearly in the amount N of adsorbed fluid, within 5 %. So, changing a mechanical parameter causes the same relative shift of N and L, within 5 %.

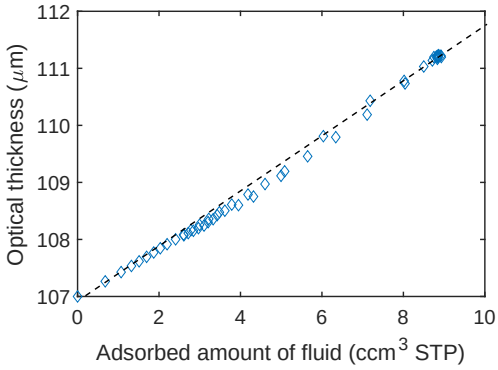

FIG. 6. Optical thickness as a function of adsorbed amount for N_2 at 77.4 K. Diamonds: experimental data, dashed line: linear fit.

REFERENCES

* rolley@phys.ens.fr, ORCID 0000-0003-1333-2541

[1] Gor, G.; Huber, P.; Bernstein, N. Adsorption-induced deformation of nanoporous materials - A review. *Applied Physics Reviews* **2017**, *4*, 011303.

[2] Vandamme, M. Coupling between adsorption and mechanics (and vice versa). *Current Opinion in Chemical Engineering* **2019**, *24*, 12–18.

[3] Gor, G. Y.; Neimark, A. V. Adsorption-induced deformation of mesoporous solids. *Langmuir* **2010**, *26*, 13021–13027.

[4] Ravikovitch, P. I.; Neimark, A. V. Density functional theory model of adsorption deformation. *Langmuir* **2006**, *22*, 10864–10868.

[5] Schoen, M.; Paris, O.; Günther, G.; Müter, D.; Prass, J.; Fratzl, P. Pore-lattice deformations in ordered mesoporous matrices: experimental studies and theoretical analysis. *Physical Chemistry Chemical Physics* **2010**, *12*, 11267–11279.

[6] Schoen, M.; Günther, G. Phase transitions in nanoconfined fluids: Synergistic coupling between soft and hard matter. *Soft Matter* **2010**, *6*, 5832–5838.

[7] Puibasset, J. Adsorption-Induced Deformation of a Nanoporous Material: Influence of the Fluid–Adsorbent Interaction and Surface Freezing on the Pore-Load Modulus Measurement. *The Journal of Physical Chemistry C* **2017**, *121*, 18779–18788.

[8] Chen, M.; Coasne, B.; Derome, D.; Carmeliet, J. Coupling of sorption and deformation in soft nanoporous polymers: Molecular simulation and poromechanics. *Journal of the Mechanics and Physics of Solids* **2020**, *137*, 103830.

[9] Neimark, A. V.; Coudert, F.-X.; Boutin, A.; Fuchs, A. Stress-Based Model for the Breathing of Metal-Organic Frameworks. *J. Phys. Chem. Lett.* **2010**, *1*, 445–449.

[10] Herman, T.; Day, J.; Beamish, J. Deformation of silica aerogel during fluid adsorption. *Physical Review B* **2006**, *73*, 094127.

[11] Espinoza, D.; Vandamme, M.; Pereira, J.-M.; Dangla, P.; Vidal-Gilbert, S. Measurement and modeling of adsorptive–poromechanical properties of bituminous coal cores exposed to CO2: Adsorption, swelling strains, swelling stresses and impact on fracture permeability. *International Journal of Coal Geology* **2014**, *134–135*, 80–95.

[12] Amberg, C. H.; McIntosh, R. A study of adsorption hysteresis by means of length changes of a rod of porous glass. *Canadian Journal of Chemistry* **1952**, *30*, 1012–1032.

[13] Grosman, A.; Puibasset, J.; Rolley, E. Adsorption-induced strain of a nanoscale silicon honeycomb. *EPL* **2015**, *109*, 56002.

[14] Prass, J.; Müter, D.; Fratzl, P.; Paris, O. Capillarity-driven deformation of ordered nanoporous silica. *Appl. Phys. Lett.* **2009**, *95*, 083121.

[15] Balzer, C.; Waag, A. M.; Gehret, S.; Reichenauer, G.; Putz, F.; Hu-sing, N.; Paris, O.; Bernstein, N.; Gor, G. Y.; Neimark, A. V. Adsorption-Induced Deformation of Hierarchically Structured Mesoporous Silica- Effect of Pore-Level Anisotropy. *Langmuir* **2017**, *33*, 5592–5602.

[16] Schappert, K.; Pelster, R. Unexpected Sorption-Induced Deformation of Nanoporous Glass: Evidence for Spatial Rearrangement of Adsorbed Argon. *Langmuir* **2014**, *30*, 14004–14013.

[17] Grosman, A.; Ortega, C. Influence of elastic strains on the adsorption process in porous materials: an experimental approach. *Langmuir* **2009**, *25*, 8083–8093.

[18] Barla, K.; Herino, R.; Bomchil, G.; Pfister, J.; Freund, A. Determination of lattice parameter and elastic properties of porous silicon by X-ray diffraction. *J. Cryst. Growth* **1984**, *68*, 727–732.

[19] Grosman, A.; Ortega, C. Influence of elastic deformation of porous materials in adsorption-desorption process: A thermodynamic approach. *Phys. Rev. B* **2008**, *78*, 085433.

[20] Eriksson, J. C. Thermodynamics of surface phase systems: V. Contribution to the thermody-

namics of the solid-gas interface. *Surface Science* **1969**, *14*, 221–246.

[21] Gor, G. Y.; Bernstein, N. Revisiting Bangham's law of adsorption-induced deformation: changes of surface energy and surface stress. *Physical Chemistry Chemical Physics* **2016**, *18*, 9788–9798.

[22] Puibasset, J. Adsorption-desorption hysteresis of simple fluids confined in realistic heterogeneous silica mesopores of micrometric length: A new analysis exploiting a multiscale Monte Carlo approach. *J. Chem. Phys.* **2007**, *127*, 154701.

[23] Naumov, S.; Khokhlov, A.; Valiullin, R.; Kärger, J.; Monson, P. A. Understanding capillary condensation and hysteresis in porous silicon: Network effects within independent pores. *Physical Review E* **2008**, *78*, 060601.

[24] Rolley, E.; Garroum, N.; Grosman, A. Using capillary forces to determine the elastic properties of mesoporous materials. *Phys. Rev. B* **2017**, *95*, 064106.

[25] Grosman, A.; Ortega, C. Capillary condensation in porous materials. Hysteresis and interaction mechanism without pore blocking/percolation process. *Langmuir* **2008**, *24*, 3977–3986.

[26] Puibasset, J.; Porion, P.; Grosman, A.; Rolley, E. Structure and Permeability of Porous Silicon Investigated by Self-Diffusion NMR Measurements of Ethanol and Heptane. *Oil & Gas Science and Technology–Revue d'IFP Energies nouvelles* **2016**, *71*, 54.

[27] Kondrashova, D.; Lauerer, A.; Mehlhorn, D.; Jobic, H.; Feldhoff, A.; Thommes, M.; Chakraborty, D.; Gommes, C.; Zecevic, J.; De Jongh, P., et al. Scale-dependent diffusion anisotropy in nanoporous silicon. *Scientific reports* **2017**, *7*, 1–10.

[28] Grosman, A.; Ortega, C. Cavitation in Metastable Fluids Confined to Linear Mesopores. *Langmuir* **2011**, *27*, 2364–2374.

[29] Pacholski, C.; Sartor, M.; Sailor, M. J.; Cunin, F.; Miskelly, G. M. Biosensing using porous silicon double-layer interferometers: reflective interferometric Fourier transform spectroscopy. *Journal of the American Chemical Society* **2005**, *127*, 11636–11645.

[30] Casanova, F.; Chiang, C. E.; Li, C.-P.; Roshchin, I. V.; Ruminski, A. M.; Sailor, M. J.; Schuller, I. K. Gas adsorption and capillary condensation in nanoporous alumina films. *Nanotechnology* **2008**, *19*, 315709.

[31] Markel, V. Introduction to the Maxwell Garnettapproximation: tutorial. *J. Opt. Soc. Am. A* **2016**, *33*, 1244–1256.

[32] Brochard, L.; Vandamme, M.; Pellenq, R. J.-M. Poromechanics of microporous media. *J.*

Mech. Phys. Solids **2012**, *60*, 606–622.

[33] Vichit-Vadakan, W.; Scherer, G. Measuring Permeability of Rigid Materials by a Beam-Bending Method: II, Porous Glass. *Journal of the American Ceramic Society* **2000**, *83*, 2240–2246.

[34] Casanova, F.; Chiang, C. E.; Ruminski, A. M.; Sailor, M. J.; Schuller, I. K. Controlling the role of nanopore morphology in capillary condensation. *Langmuir* **2012**, *28*, 6832–6838.

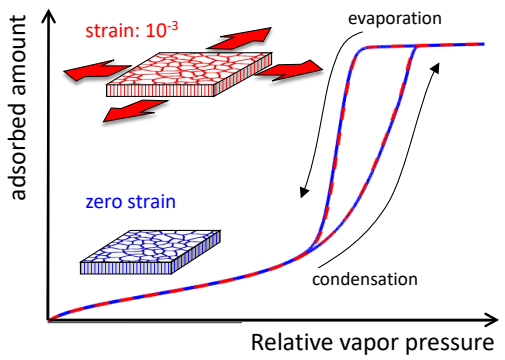

FIG. 7. For Table Of Content Use Only